Identification of Rip Current Images Using Artificial Intelligence

Mickey Yang[1], Ethan Meng[2], Connor Wu[3]

[1]Beijing No.80 High School, qiaoyang172@163.com

[2]Beijing No.80 High School, darkest_destiny@163.com

[3]Beijing No.80 High School, connorwyx4@gmail.com

Beijing No.80 High School

Mrs. Yao W. Teacher

September 15th 2024

Abstract

Rip currents pose significant hazards to beachgoers, often catching untrained individuals unaware and leading to dangerous situations. The research aims to develop an effective method for detecting rip currents using artificial intelligence, thereby enhancing beach safety. The method involves training a binary classification model on aerial images of the ocean, categorizing them into those with rip currents and without rip currents. Data augmentations such as cutting, rotating, and flipping the image are employed so that the generalization ability of our model could be enhanced. We utilized Multi-Layer Perceptron classifiers, achieving a accuracy of 73.9% initially on testing set, and an accuracy of 92.5% after applying a confidence threshold. The integration of the model with a Tello Talent Robomaster TT drone introduced significant flexibility and efficiency, with an average processing time of 3.09 milliseconds per 1000 images. With a True Positive Rate (TNR) of 93.06% and True Negative Rate (TNR) of 91.10%, the model also demonstrated relatively high performance. This innovative approach of integrating AI with rip current proves to be flexible, efficient, and effective making a significant contribution to beach safety.

Key words: Rip current; Artificial intelligence; Binary classification; Beach safety; Artificial neural network; Marine environmental monitoring

Table of Contents

Identification of Rip Current Images Using Artificial Intelligence

Rip currents are powerful, narrow channels of fast-moving water running from a beach back to the open ocean, sea, or lake, usually sustains for several minutes. Rip current can move up to 8 feet per second (more than 2 meters per second), which is much faster than even Olympic swimmers. They are usually caused by the fragmented tides created by radiation stress in water waves. The diagram in Figure 1 illustrates the anatomy of a rip current.

Figure 1

Anatomy of the rip current

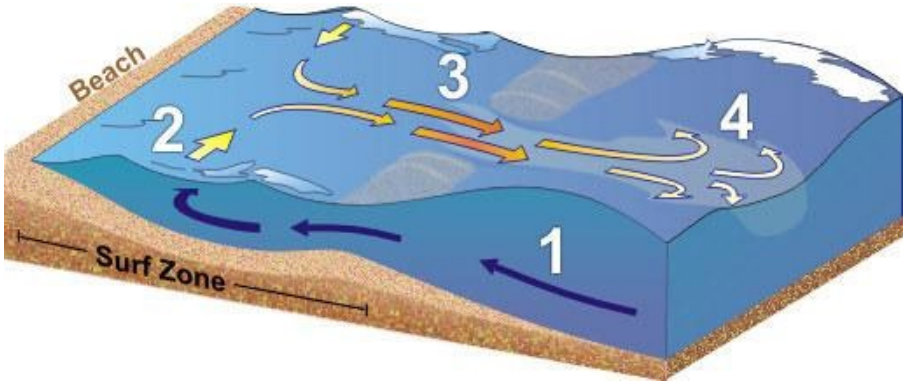

Note. This image was acquired from the website of National Oceanic and Atmospheric Administration (NOAA). (*Rip Currents*, 2023)

Hazard of Rip Currents

Rip currents present a significant danger due to the general public's lack of awareness or inability to recognize these potentially lethal oceanic phenomena, often resulting in hazardous situations for unsuspecting swimmers. Typically, surfers often show themselves as calm areas in a sea of waves and this may deceive people into thinking that these are safe places. In essence, however, these tranquil zones are the most dangerous where strong currents create significant hazard. The untrained eye will not straightforwardly or hastily notice the subtle visual indicators of the presence of a rip current like watery tones, wave patterns or even foam moving outwards together with seaweed or debris (see Figure 2).

Figure 2

Examples of rip current patterns (Automated Rip Current Detection, n.d.*)*

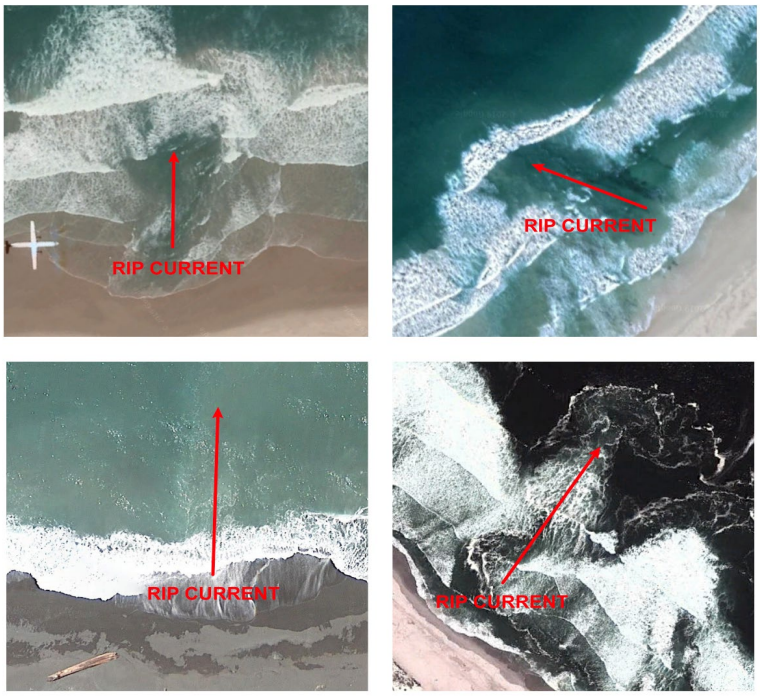

The high incidence of rip currents poses a significant danger to the general public, as evidenced by information from the National Oceanic and Atmospheric Administration (*Rip Currents*, 2023). Rip currents were responsible for more than 80% of water rescue cases carried out by lifeguards across America in 2023. This means that approximately 90 out of 98 times someone had to be saved from drowning, it was due to rip currents (US Department of Commerce, n.d.). Moreover, the reports coming from Florida Panhandle reveal that rip tides cause 60 percent of the deaths around the Great Lakes thus demonstrating their fatal nature (Florida Panhandle, 2023).

This magnifies the issue because rip currents can hardly be predicted making it difficult for people to spot them easily. It should also be remembered that they can form and disappear quickly hence giving no time for immediate warnings or closely monitoring all potential danger zones by beach safety staff. This unpredictability necessitates the need for efficient alert systems meant to protect members of the general public.

Given these challenges, there is a pressing need for advanced technological solutions to aid in the identification and monitoring of rip currents. AI-based models integrated with drones, like the system we propose, offer a promising approach to enhance beach safety. By providing real-time, accurate detection of rip currents, such systems can alert both the public and lifeguards to potential hazards, thereby reducing the risk of accidents and saving lives.

Literature review

Hazard and Influence.

Rip currents have been reported as the most hazardous safety risk to beachgoers (Rampal et al., 2022). In China, accumulated Chinese surf zone fatalities were reported more

than marine disaster casualties over the recent ten years. The surf zone accident has a high occurrence frequency in the southern regions and peaks from July to August (Zhang et al., 2021). In Australia, rip currents are responsible for more deaths than hurricanes, floods, and tornados combined ("Methodology for Prediction of RIP Currents Using a Three-Dimensional Numerical, Coupled, Wave Current Model," 2011). Governments are concerned about the negative social and economic influence caused by the rip current. Many countries have established operational frameworks across various organizational levels on rip current prevention, including risk investigation, data-driven forecasting, beach safety improvement, and public awareness (Zhang et al., 2021). Despite warning signs and educational campaigns, many beachgoers and visitors still do not know how to reliably and efficiently identify and localize rip currents, and this coastal process still poses serious threats to beach safety (Pitman et al., 2021). This also extends to lifeguards, who, because of the oblique angle they observe the ocean, can struggle to identify certain rip currents, especially when the coastal morphology is complex.

Recent Study

As a public safety hotspot, the rip current has long been of great research interest in its mechanism, characteristics, and prediction. (Zhang et al., 2021b) Many practical approaches are adopted in the study of the rip current, such as scaled experiment, numerical simulation, remote image interpretation, onsite observation and measurement simulation, remote image interpretation, onsite observation and measurement (Castelle et al., 2016b). Owing to the intrinsic instability of the rip current, accurate prediction of its exact occurrence is not feasible at present (Zhang et al., 2021b).

CNN and AI Predictions

An interpretable AI was brought by the scientists to make predictions on and localize rip currents. They also emphasize some of the advantages of supervised learning using deep learning techniques such as Convolutional Neural Networks (CNNs) which are able to learn through experience, learn complex dependencies and features in order to get a set of model weights/parameters that give out maximum accuracy (Rampal et al., 2022).

In short, rip currents indicate grave safety concerns. They influence beachgoers, coastal communities, and local governments profoundly. Recent studies mainly focused on hazards and social impacts while only a few provided plausible solutions towards severe problems caused by rip currents.

While the use of interpretable AI and CNN is an effective and unique method for detecting and predicting rip currents, the authors failed to offer any guidance on how to apply this technique in practice.

Methodology

To address the problem of effectively detecting rip currents and enhancing beach safety, we developed an AI-based model integrated with drone technology.

Data Acquisition and Preprocessing Pipeline

Image Acquisition

The first step is to collect a dataset of images representing near-shore conditions for training. A total of 2484 images, including scenarios of both rip currents (1781 images) and

non-rip currents (703 images), were acquired from the database (Castelle et al., 2016b), provided by (de Silva et al., 2021), to build a reliable model for classifying rip currents. These images are high-resolution aerial images from Google Earth (Rampal et al., 2022). The 2484 images were split into two parts. One, taking up 80% of the total dataset, was used as the training set. This part contains 1425 (contains rip currents) + 562 (no rip currents) = 1987 images. The other part, which contains 356 (contains rip currents) + 141 (no rip currents) = 497 takes up 20% and was used as testing set. No validation set was established due to the relatively limited amount of data.

Data Augmentation

In this study, we implemented a data augmentation pipeline to increase robustness and generalization of our neural network model. This is achieved through the diversity attained in the training dataset by applying various transformations on the original images hence generating new examples with additional manual labeling.

Our augmentation strategy involves several techniques. First, we apply random rotations to the images by multiples of 90 degrees. This aids the model in identifying objects without considering their orientation. We also perform random cropping and resizing, which introduces variability in the scale and viewpoint of the images. Additionally, random horizontal flips are applied to the images to ensure that the model learns to identify features from both left and right perspectives. The process of augmentation was automated by a custom Python script utilizing OpenCV. A few examples of augmented images will be shown later.

Four augmentations on training set with no rip currents and four augmentations on image dataset with rip currents were done. There are a total of 7948 images in the training set, which is calculated by multiplying 1986 by 4. 7948 (training set after augmentation) + 497 (testing set)

= 8445 images were actually used in the model training.

Table 1
Training, testing, and rip current existence dataset detail

	Training	Testing	Total
With Rip Current	1425	356	1781
With No Rips Current	562	141	703
With 4 Augmentations	7948	497	8445

Dataset Preparation

Since the dataset has images with resolution varying from 234×234 to 1094×1322, after augmenting the images, it is essential to standardize them in order to maintain uniformity concerning input format for the model. The resizing process was done using OpenCV library and images were adjusted to a fixed resolution of 20 pixels by 20 pixels, gaining the advantage of lowering computational effort during training process of the model. Along with this, these images are turned into grayscale through OpenCV. Converting images into grayscale simplifies information content and reduces data into one channel. This sort of operation focuses on structural characteristics instead of color changes and makes learning more efficient and better model training possible.

Figure 3

Image of the rip current before and after the augmentation

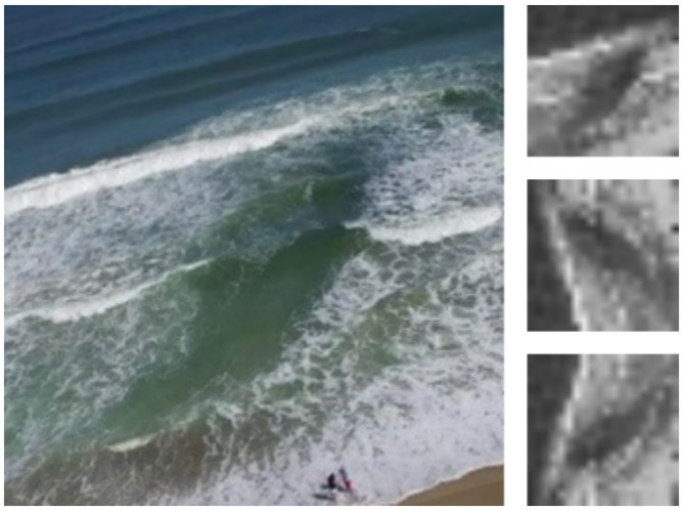

Note. On the left is the original image and on the right are three different images after augmentations and dataset preparation

Preprocessing

After that, every image was translated into a Comma-Separated Value (CSV) file so that the model could be trained. This stage required converting 2D array of pixel values into one row of CSV files. Each cell sequentially records the grayscale value of one pixel thus resulting in a 1-row sequence having 400 columns. In every row's first column, labels were added which show if rip currents are there (1) or not there (0). The binary classification (labeling) of the training dataset has already done when we acquired the images. The machine learning model was trained using this binary classification to enable it to accurately differentiate between rip current and non-rip current.

Model Training

Model Selection

In this project, we utilize Scikit-Learn Library's MLPClassifier, which serves as a Multilayer Perceptron Classifier for our neural network model. The Multi-Layer Perceptron Classifier is highly fitting for this purpose because it can deal with complicated patterns and relationships within the data using artificial neural network principles. The option to choose MLPClassifier was based on its being tested in recognition tasks using images as well as its ability to optimize performance after adjusting these parameters (Gong, 2022; *Sklearn.neural_network.MLPClassifier*, n.d.).

Architecture and training parameters

The model's architecture consists of a solitary hidden layer with **60** neurons. ReLU activation function was employed for hidden layer which nonlinearity reveals itself inside a web of complex patterns that emerge out of the given facts. The SoftMax activation function

was imployed at output layer due to its excellent performance in classification tasks (Zhang et al., 2021).

The model is trained with the 'Adam' optimizer which is an efficient version of stochastic gradient descent that adapts learning rate for each parameter (Gong, 2022; Kingma & Ba, 2014). The learning rate for the 'Adam' optimizer has been established as 0.001. Optimizing this way means we are trying to minimize binary cross-entropy loss which makes it suitable for binary classification tasks.

To ensure reproducibility, random_state = 1 is used as a random seed. The maximum number of iterations for the model training has been specified as 150, allowing weights to be updated through backpropagation until convergence or the iteration limit is reached.

Figure 4

Diagram illustrating the structure of the neural network, with number of nodes not accurately represented

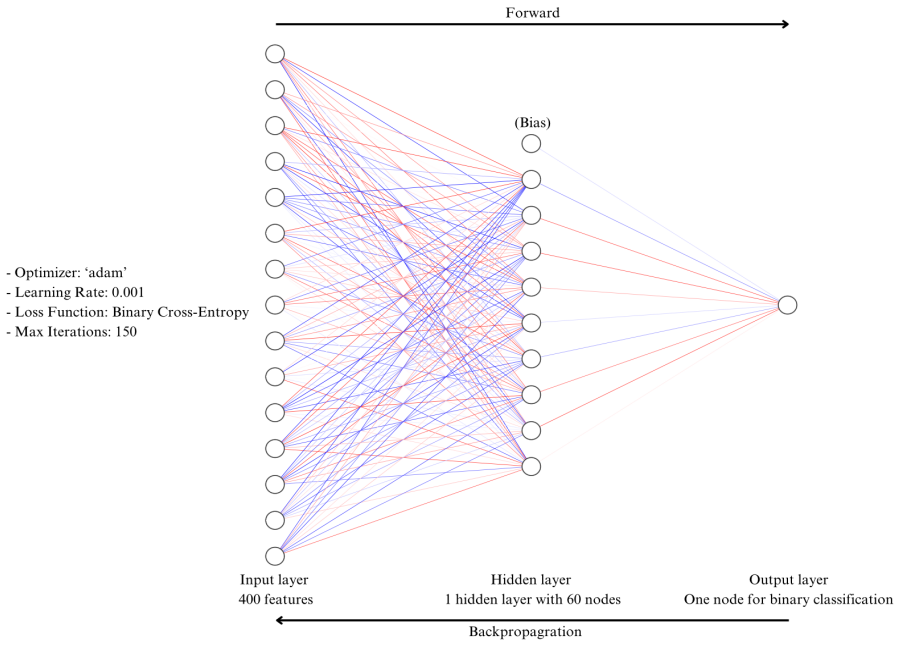

After conducting four augmentations on the testing image dataset inclusive of both rip currents and no rip currents, a combined total of 7948 augmented images were included in the training set.

Result

Performance Metrics

When assessing the performance of our binary classification model, we have taken into account multiple important metrics, including accuracy, true negative rate(TNR), and true positive rate(TPR).These measures give a clear reflection on how well the model distinguishes between images that have rip currents from those that do not have them.

The accuracy means the proportion of number of correctly classified instances over the that of total instances in the dataset. The accuracy of our model was **82.8%** on the training set and **73.9%** on the testing set. This indicates that even on unseen data our model performs relatively good, maintaining high accuracy levels from training through testing.

The True Negative Rate (TNR) quantifies the percentage of true negative instances accurately classified by the model. The model reached a True Negative Rate (TNR) of **0.62** in our testing set. This indicates that **62%** of the images lacking rip currents were accurately categorized. The True Positive Rate (TPR) calculates the percentage of true positives accurately identified by the model. On the testing set, the TPR was **0.75**, indicating that **75%** of the images with rip currents were correctly classified.

Figure 5

Examples of FP, TN, TP and FN classifications

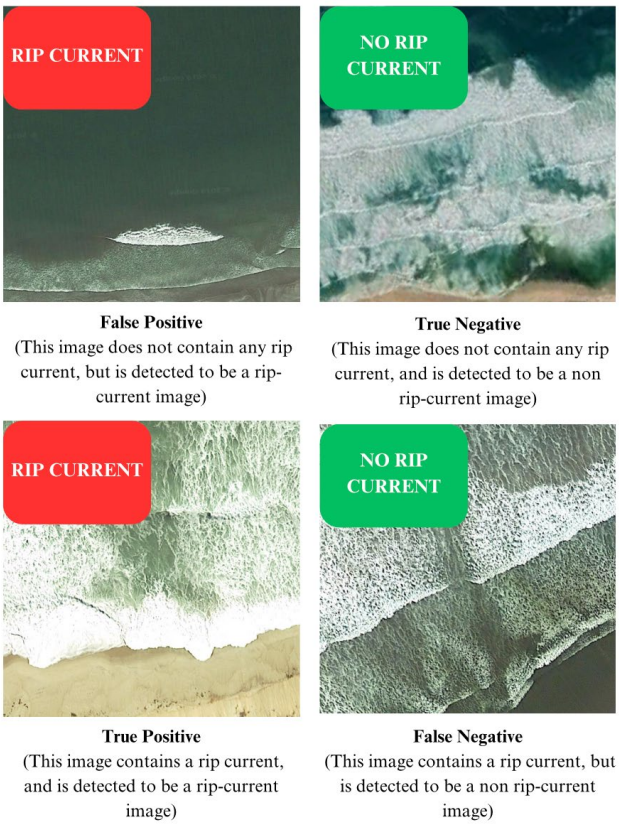

False Positive
(This image does not contain any rip current, but is detected to be a rip-current image)

True Negative
(This image does not contain any rip current, and is detected to be a non rip-current image)

True Positive
(This image contains a rip current, and is detected to be a rip-current image)

False Negative
(This image contains a rip current, but is detected to be a non rip-current image)

The time it took to train the model was also a crucial factor. The total time taken to train the model was **6.48** seconds, highlighting the efficiency of the training process. This quick training time is particularly advantageous when dealing with large datasets or when frequent model updates are required. This aspect will be further elaborated on in subsequent sections. Also, it takes only **25.97** milliseconds to run both of the training and the testing set, which is **3.09** milliseconds only for **1000** images on average. This fast runtime ensures that the model can be used in real-time applications where rapid image classification is essential.

Rip Current Classification System Integration with Drone

Setting Confidence Threshold

When it comes to implementing the rip current classification system, we considered tuning the confidence threshold to optimize the product of True Positive Rate (TPR) and True Negative Rate (TNR) in our subsequent research. With 0.75 initial TPR and 0.62 TNR, we tried to arrive at a threshold that could enhance overall model performance.

To find the ideal threshold level, we calculated various TPRs, TNRs and measured TPR × TNR values. The objective was to determine the optimal point at which this product achieves the highest balance between true positive and true negative rates. In order to set a confidence threshold, one needs to calculate probabilities of $\boldsymbol{n}$ true positives or $\boldsymbol{n}$ true negatives occurring among $\boldsymbol{\alpha}$ trials, then sum up all probabilities greater than $\boldsymbol{n}$. That gives us both TPR and TNR values. If we wish to maximize them both then we must compare the value of **TPR × TNR** since they are equivalent in importance. We found out that by having $\boldsymbol{n}$ set at approximately $\mathbf{0.69 \times \alpha}$, we get the highest value of TPR and TNR.

Table 2

TPR, TNR and TPR time TNR values at different thresholds

Positive accuracy		0.75	True Postive Rate (TPR)	Negative accuracy		0.62		True Negative Rate (TNR)	TPR × TNR
trials (*n*)	100	probability		trials	100	probability	n and above		
0		6.223E-61	0.955403675	0		9.5139E-43	0.128001035	0.871998965	0.833111015
1		1.8669E-58	0.955403675	1		1.5523E-40	0.128001035	0.871998965	0.833111015
2		2.7724E-56	0.955403675	2		1.2537E-38	0.128001035	0.871998965	0.833111015
3		2.7169E-54	0.955403675	3		6.6818E-37	0.128001035	0.871998965	0.833111015
… …									
68		0.02475256	0.955403675	68		0.03900174	0.128001035	0.871998965	0.833111015
69		0.03443835	**0.930651111**	69		0.02951161	0.088999295	**0.911000705**	**0.847823818**
70		0.04575381	0.896212761	70		0.02132381	0.059487681	0.940512319	0.842899142
… …									
97		1.9208E-09	2.10817E-09	97		6.4574E-17	6.79068E-17	1	2.10817E-09
98		1.764E-10	1.87408E-10	98		3.2252E-18	3.33325E-18	1	1.87408E-10
99		1.0691E-11	1.10114E-11	99		1.0631E-19	1.08041E-19	1	1.10114E-11
100		3.2072E-13	3.2072E-13	100		1.7345E-21	1.73448E-21	1	3.2072E-13

Note. Only a part of the table was shown due to space limitation. Full table could be freely accessed at https://github.com/MickeyYQA/rip_current-appendix (accessed on June 30, 2024).

Figure 6

Line chart - TPR times TNR values at different confidence threshold

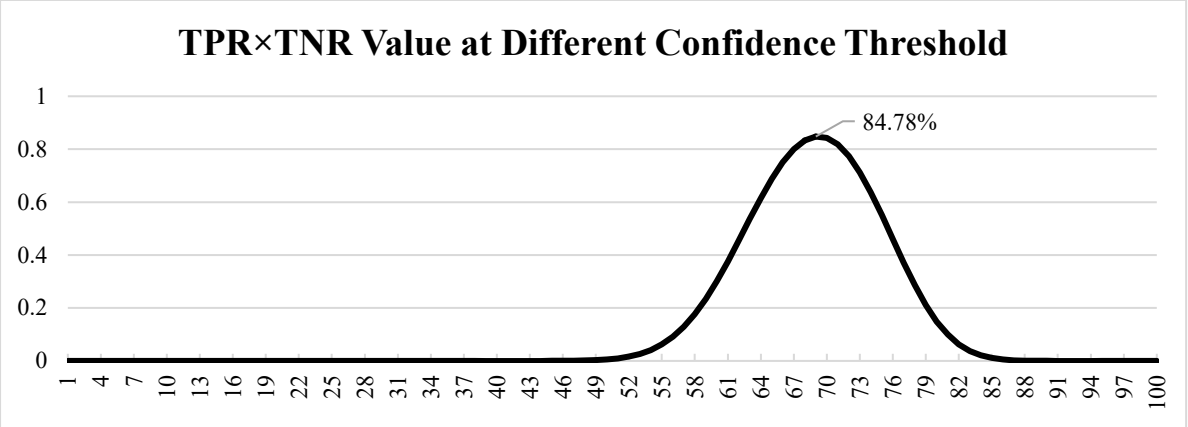

From the analysis presented in the table above, the TPR and TNR values were computed for different confidence levels. The product of TPR and TNR was used as the benchmark to evaluate the performance at each threshold. As shown in the table, the threshold of 69 trials yielded the highest TPR × TNR value of **84.78%**, with a corresponding TPR of **93.06 %** and TNR of **91.10 %**. This indicates that at this threshold, the model achieves a near-optimal balance between correctly identifying images with and without rip currents.

Given that TPR is 93.06% while TNR is 91.10% under the 0.69 confidence threshold, the overall performance accuracy could be calculated. By referring to the formula

$$Accuracy = (TPR \times \frac{P}{N+P}) + (TNR \times \frac{N}{N+P})$$

we will get the TPR = 0.9306, TNR = 0.9110, P (Positive dataset size) = 1781, N (Negative dataset size) = 703, we finally got the overall accuracy under the confidence threshold of 0.69:

$$Accuracy = (0.9306 \times 0.7169) + (0.9110 \times 0.2830) = 0.9249$$

Furthermore, after comparing the result of different $\boldsymbol{\alpha}$ values, we decided to set it to 100, which gives us a high classification accuracy and low classification interval of around 1.3 seconds. This means that the drone could classify 100 images in 1.3 seconds to get one result with accuracy of **92.49 %**. This time interval was got by testing in real situations w

Figure 7

Sketch of the process of drone integration.

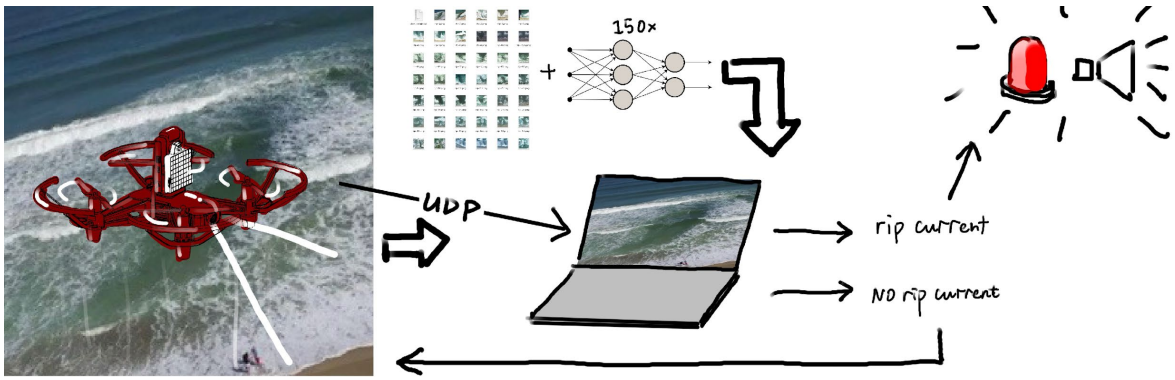

Real-time Image Transmission

In addition to the implementation of AI, our team has also decided to use drone for the coastline footage. With the usage of drone taking footage from the air, we can achieve a real-time detection along the coastline and cover much more area. By doing this research, we built a system that can actively and reliably detect rip currents along coastlines to prevent fatalities happening due to the rip currents.

In our research, the model was integrated with the drone to demonstrate the flexibility and adaptability of this approach. Since this rip current classification system was integrated with the “Tello Talent Robomaster TT” drone, real-time image transmission capabilities were established using the features of the Tello drone development kit. This was achieved by communicating using UDP (User Datagram Protocol) which allowed the drone’s camera to send live videos to a computer (*RoboMaster TT - Specifications - DJI*, 2024). Low latency

transmissions that are essential for real time processing and classification provided by UDP.

Image Preprocessing

The images of the camera of the drone were resized to 10x10 pixels and converted to gray scale in order to match them with training data. The test set was expected consist of pictures, whose dimensions or format were not changed for accurate predictions when applied in a real-world scenario.

Model Inference

Processed images such as these ones are passed through a pre-trained ANN model to detect rip currents. These images processed will be fed into this model at inference time and outputs which indicate whether it might lead to rip current events or not. Thus, seamlessly integrating live video streams would enable instant feedback on possible dangerous issues, such as rip currents.

Enhancing Prediction Accuracy

In an effort to make more accurate predictions of rip currents, a customized method was designed and implemented. The function predicts rip current presence multiple times for every image and then combines the answers to create better concepts as well as more reliable results. Precisely, each image is subjected to 100 predictions by the model. Where 69 or more of these predictions indicate that there is a rip current, the system confirms this fact. This confidence threshold empirically achieved a balance between sensitivity and specificity based on initial analysis.

Result Display

To display immediate and clear feedback in relation to the classification outcomes, we created a graphical user interface using OpenCV. If it detects a rip current (which means it has made 100 predictions where the confidence levels are higher than 82%), then this interface will pop-up a window displaying "RIP CURRENT" with a red background if a rip current is being classified, and "SAFE" with green background color in case no rip current is being classified.

Figure 8

Rip currents classification user interface demonstration

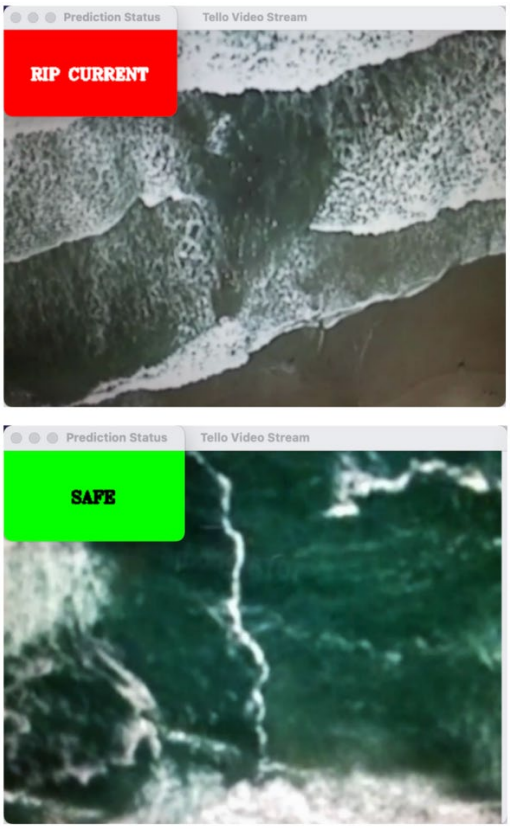

Note. Image above demonstrates the GUI where the camera data received from the drone is shown, and the true prediction of that rip current exists is shown on the left, while the true

prediction of that rip current does not exist is shown on the right. This screen capture shows the real user interface being tested, not a simulated demonstration.

Testing and Validation Methodology

The integrated system underwent comprehensive testing and validation through the use of simulated and real-world test scenarios. Simulated testing was done through controlled conditions whereby pre-recorded images and video feeds were utilized to check that the system functioned well or not. But we are unable to test its performance in real beach environments due to some external limitations.

Discussion and Conclusion

Methods Comparison

The database we used was sourced from previous research conducted by de Silva et al. (2021) and his colleagues. It is a large dataset with many pictures and videos, randomly containing rip currents which can be used to train the artificial intelligence module. The former work Rampal et al. (2022) used CNN and Interpretable AI that were employed in classifying and localizing rip currents. Both these two techniques have an improving effect on the overall prediction rate. Additionally, Interpretable AI has the capability of identifying waves in videos or images making predictions more intuitive.

However, when this model is deeply trained with available data, it makes CNN module highly dependable. This implies that it has the ability to learn intricate patterns and features at high accuracy. In another study, Faster R-CNN was combined with custom temporal aggregation phase for efficient recognition of rip currents within a defined area. These

technologies have been previously applied in other studies and achieved impressive results.

Nevertheless, there are still limitations in these approaches. CNN method needs costly hardware as well as huge amounts of data for training the AI system. Therefore, it makes this process more complex hence making it slow to proceed effectively.

On the other hand, our program employed modules that were quite efficient relative to the earlier one. Also, our programs afford relatively good detection of rip currents. The previous study by Rampal et al. (2022) had an accuracy rate of 89% using their test videos, while our modules initially gave 74% on testing sets but rose to 93% after adjusting confidential threshold.

Contrastingly, the work of de Silva et al. (2021) achieved a total accuracy of 98% but framing during detection is a requirement for the method hence making it inflexible and less effective during detection. In addition, this method is not capable real-time operation and often times doesn't fit well with mobile devices as opposed to our programs which can be used on drones promptly.

Our program has several advantages over current methods discussed in previous studies. That said, there are few limitations in relation to our method. Our systems have never been tested under actual conditions such as those near sea shores or beaches. This might be a significant factor because wind and rain could affect the field of view of cameras due to bad weather situations among others. Furthermore, we employed drones with restricted altitude and flight range in this research project, with the exception of using drones with limited flight distances, which are essential for assessing the detection area's dimensions.

Conclusions

Our study utilizes visual images and videos from the “Tello Talent Robomaster TT” drone for rip current detection. Data acquisition and preprocessing algorithm got 2484 nearshore condition images in the system and data augmentation got 7948 images for training. These images were then adjusted to 400 pixels and converted to grayscale. For module training, we employed MLP algorithms having an architecture with one hidden layer of 60 neurons and ‘Adam’ solver for training.

Likewise, numerous other studies have also used AI to detect rip currents along coastal areas. However, they either have to make a bounding box in the pictures or they are not accurate enough. The demand for making bounding boxes highly affected the diversity of videos that in turn influenced the flexibility of our method overall.

The method presented addresses these limitations and provides a mobile way of detecting rip currents. After carefully weighing the results of the individual tests, we achieved an accuracy of 74% on testing data and 93% after adding a confidential threshold. Although this accuracy is lower than that of the study presented by de Silva et al. (2021), it’s relatively more flexible than other previous studies. Aside from that, drones are employed to further test the viability of the method. The outcome, although not tested in real scenes, is expected to be similar to the initial accuracy based on the videos in the database.

Future Prospects

The present study looks forward to promoting the practicability of this method further after its presentation here. To test if drones can be used in coastal areas, drone will be used on nearby coastline while assessing environmental factors for detection purposes. This is because the

quality captured by these records may easily be marred by wind and rain conditions.

Collaborating with the local government and passing information to lifeguards would be another way of using an alert mechanism to alert beachgoers and tourists in case rip currents occur. The program's interface will also be modified so as to enable users have access to real time rip current information and safety results through mobile applications and web platforms.

The other thing is that the development of advanced image processing techniques for extracting more informative features from live video feed can be examined to improve upon the accuracy of rip current detection in the future.

Data Availability Statement

The data utilized for training the AI-driven model can be freely accessed at the following link: https://sites.google.com/view/ripcurrentdetection/download-data (accessed on June 30, 2024), provided by de Silva et al. (2021). Moreover, the code mentioned in this paper is available for free download at https://github.com/MickeyYQA/rip_current_detection (accessed on June 30, 2024).

Acknowledgement

We extend our heartfelt gratitude to all those who have contributed to the completion of this research project. First and foremost, we express our sincere appreciation to Mrs. Yao Wang, a first-level teacher from Beijing No.80 High School, for her invaluable guidance throughout the course of this study. Mrs. Wang generously shared her expertise in academic writing standards, research methodologies, and scholarly norms, although her mentorship was provided on a voluntary basis.

Our team comprised three dedicated students: Mickey Yang, Ethan Meng, and Connor Wu. Under the supervision of Mrs. Wang, the topic of our research emerged from collaborative brainstorming sessions among the students. The acquisition of data relied upon databases publicly accessible through the work of De Silva et al., skillfully sourced by Connor Wu. The algorithmic design was meticulously executed by Mickey Yang, while Ethan Meng played a pivotal role in refining and enhancing the manuscript during the editing phase. The collaborative effort culminated in a comprehensive research report, with specific contributions as follows: Ethan Meng led the drafting of the Introduction section, Mickey Yang and Ethan Meng jointly handled the Methodology, and Connor Wu took charge of the Discussion and Conclusion sections.

Throughout the entire research process, we encountered various challenges, each of which was met with collaborative problem-solving. These experiences have enriched our understanding and deepened our appreciation for the complexities inherent in scientific inquiry.

Once again, we express our heartfelt thanks to Mrs. Yao Wang for her guidance and support, and to each member of our team for their diligent efforts and unwavering commitment to excellence.

References

Automated Rip Current Detection. (n.d.). Sites.google.com. https://sites.google.com/view/ripcurrentdetection/home

Brander, R., Dominey-Howes, D., Champion, C., Del Vecchio, O., & Brighton, B. (2013). Brief Communication: A new perspective on the Australian rip current hazard. *Natural Hazards and Earth System Sciences*, *13*(6), 1687–1690. https://doi.org/10.5194/nhess-13-1687-2013

comp.ai.neural-nets FAQ, Part 2 of 7: LearningSection - What is a softmax activation function? (n.d.). Www.faqs.org. http://www.faqs.org/faqs/ai-faq/neural-nets/part2/section-12.html

de Silva, A., Mori, I., Dusek, G., Davis, J., & Pang, A. (2021). Automated rip current detection with region based convolutional neural networks. *Coastal Engineering*, *166*, 103859. https://doi.org/10.1016/j.coastaleng.2021.103859

Dérian, P., & Rafaël Almar. (2017). Wavelet-Based Optical Flow Estimation of Instant Surface Currents From Shore-Based and UAV Videos. *IEEE Transactions on Geoscience and Remote Sensing*, *55*(10), 5790–5797. https://doi.org/10.1109/tgrs.2017.2714202

"Florida PanHandle." FloridaPanhandle.com, 30 June 2023, floridapanhandle.com/blog/rip-current-statistics/

Gong, C. (2022). *Introduction to visual perception*. Chemistry Industry Press Co., Ltd.

Haller, M. C., Honegger, D., & Catalan, P. A. (2014). Rip Current Observations via Marine Radar. *Journal of Waterway, Port, Coastal, and Ocean Engineering*, *140*(2), 115–124. https://doi.org/10.1061/(asce)ww.1943-5460.0000229

Kingma, D., & Ba, J. (2014). Adam: A Method for Stochastic Optimization. *Computer Science*. https://doi.org/10.48550/arXiv.1412.6980

Liu, B., Yang, B., Masoud-Ansari, S., Wang, H., & Gahegan, M. (2021). Coastal Image Classification and Pattern Recognition: Tairua Beach, New Zealand. *Sensors*, *21*(21), 7352–7352. https://doi.org/10.3390/s21217352

Methodology for Prediction of Rip Currents Using a Three- Dimensional Numerical, Coupled, Wave Current Model. (2011). *CRC Press EBooks*, 103–122. https://doi.org/10.1201/b10916-10

Mucerino, L., Carpi, L., Schiaffino, C. F., Pranzini, E., Sessa, E., & Ferrari, M. (2020). Rip current hazard assessment on a sandy beach in Liguria, NW Mediterranean. *Natural Hazards*, *105*(1), 137–156. https://doi.org/10.1007/s11069-020-04299-9

Pitman, S. J., Thompson, K., Hart, D. E., Moran, K., Gallop, S. L., Brander, R. W., & Wooler, A. (2021). Beachgoers' ability to identify rip currents at a beach in situ. *Natural Hazards and Earth System Sciences*, *21*(1), 115–128. https://doi.org/10.5194/nhess-21-115-2021

Rampal, N., Shand, T., Wooler, A., & Rautenbach, C. (2022). Interpretable Deep Learning Applied to Rip Current Detection and Localization. *Remote Sensing*, *14*(23), 6048. https://doi.org/10.3390/rs14236048

Rip Currents. (2023). Noaa.gov. https://www.noaa.gov/jetstream/ocean/rip-currents#:~:text=Rip%20currents%20are%20powerful%2C%20channeled%20currents%20of%20water

RoboMaster TT - Specifications - DJI. (2024). DJI Official. https://www.dji.com/cn/robomaster-tt/specs

Salama, N. M., Iskander, M. M., El-Gindy, A. A., Nafeih, A. M., & Hossam El-Din M. Moghazy. (2023). Hydrodynamic Simulation of Rip Currents Along Al-Nakheel Beach, Alexandria, Egypt: Case Study. *Journal of Marine Science and Application/Journal of Marine Science and Application*, *22*(1), 137–145. https://doi.org/10.1007/s11804-023-00320-2

sklearn.neural_network.MLPClassifier. (n.d.). Scikit-Learn. https://scikit-learn.org/stable/modules/generated/sklearn.neural_network.MLPClassifier.html#

US Department of Commerce, N. (2023). *Surf Zone Fatalities in the United States in 2022: 5*. Www.weather.gov. https://www.weather.gov/safety/ripcurrent-fatalities

Zhang, Y., Huang, W., Liu, X., Zhang, C., Xu, G., & Wang, B. (2021). Rip current hazard at coastal recreational beaches in China. *Ocean & Coastal Management*, *210*, 105734.

https://doi.org/10.1016/j.ocecoaman.2021.105734